Effective Thermal Management of Multiple Electronic Components

Chun Sheng Yu, Shung Wen Kang, Ming Tai Weng

Department of Mechanical and Electro-Mechanical Engineering, Tamkang University
151 Ying-Chuan Rd., Tamsui, 25137, Taiwan, R.O.C.
Tel: 886-2-26215656 Ext.2613; Fax: 886-2-26209745
892340067@s92.tku.edu.tw
swkang@mail.tku.edu.tw
ted.weng@foretherma.com.tw

ABSTRACT

The objective of this paper is to provide an effective and accurate analytical solution to compute the spreading thermal resistance of a vapor chamber thermal module, as well as the surface temperatures and the heat flux distributions at the heating surface. The analytical solutions are expressed in a reduced unit system with the governing parameters of the corresponding distance between heat sources, dimensionless plate thickness of the vapor chamber. This paper also presents vapor chamber temperature distribution, and it is correlation to heat source sizes, hence, spreading thermal resistance decreases with the increasing lateral length. There is the obvious difference between spreading thermal and conductive thermal resistance as lateral length is disproportion to heating area. Therefore, spreading thermal resistance is an important factor when design the thermal solution of a high density chipset power, and it caused high temperature in heat sources by embedded a thinner heat sink base. According to Fourier conductivity theorem, spreading thermal resistance is disproportion to sink base, then thermal resistance is not only parameter for vapor chamber module design, it needs to consider spreading resistance of vapor chamber and fin performance for cooling LEDs array, in order to prevent mismatch on numerical analysis and mathematical calculation. Thermal simulation is used as a design tool, and it is close to experimental data. The difference is within 5.9%, and it presents a precise result.

Key words: vapor chamber, multiple heat sources, spreading thermal resistance

NOMENCLATURE

A	Heat source size, m^2
Ac	Contact area of non-circular plate, m^2
Aeq	Equivalent size of a single heat source, m^2
As	Base pate area of non-circular plate, m^2
a	Heat source radius, m
b	Base plate radius, m
d	Distance between heat sources, m
h	Convection heat transfer coefficient, $W/m^2 \cdot K$
k	Thermal conductivity, $W/m \cdot K$
l	Length of base plate, m
m	Length of heat source, m
m_{eq}	Length of a single equivalent heat source, m
Q	Heat flow rate, W
R_{1D}	One dimensional thermal resistance, • •/W
R_s	Spreading thermal resistance, • •/W
R_t	Total thermal resistance, • •/W
T	Temperature, • •
t	Base plate thickness, m

Subscripts

f	External air
ave	Average value
b	Bottom surface of base plate
c	Contact area
max	Maximum value
s	Top surface of base plate

1 INTRODUCTION

This study focuses on recent applications of latent heat transfer with phase change transmission is constantly used as heat-transport devices because of the superiority of transferring heat within low temperature differences. Recently, by stable capability and reliability of vapor chambers fabrication, thus, the vapor chambers are applied on the electronic cooling. In the proposed thermal design model, vapor chamber works as a high conductivity interface between heat sources and heatsink, so the local temperature distribution and the heat spreading effect can be therefore investigated. Furthermore, the calculated results are in line with the results in previous literatures and the experiments conducted in this study.

Experimental comparisons between copper, aluminum plates and a vapor chamber having the same thickness have been also summarized. The spreader plates integrated with a plate-fin heatsink are tested in a wind tunnel. For small footprint heat sources, the vapor chamber shows a lower thermal resistance and much uniform temperature distribution than the metal plates. Then, the heatsink integrated with the vapor chamber is simulated by using numerical model. In order to obtain more accurate calculation domain, the heating block and insulation are also considered in simulation boundary conditions. These available analysis models are simulated to real applications, the maximum difference of the hot spot temperature rises between the simulation and analytical result is 5.9 %. Additionally, a steady state three dimensional heat conduction equation is analytically solved by using separation of variables. The temperature distribution within a partially heated rectangular plate is solved and the spreading thermal resistance is also obtained.

By adapting the ideas of isotropic or anisotropic heat spreading, the equivalent heat source by multiple heat sources and effective thermal conductivities of the vapor chamber have been calculated. The axial conductivity of the vapor chamber is around 48.74 W/m-K, but the lateral length conductivity is more than ten times of the axial conductivity [1]. The high lateral length conductivity can sufficiently enhance the heat spreading along the lateral direction, and thereby resulting in a lower total thermal resistance. Combining into the whole module simulation, the surface temperature distribution is similar as that obtained by numerical model. In additions, the thermal spreading resistances have also been analytically investigated. An anisotropic method to calculate the effective thermal conductivities of vapor chamber is also proposed [2].

2 Fundamental theorem

2.1 Spreading thermal resistance

Spreading resistance caused by mismatch contact area (footprint) between heat source and heatsink base. Efficiency of thermal dissipation changes with the size of heat source as electronic component generates constantly power transmission [3]. The smaller size of heat sources, the higher thermal density on heatsink, which accumulated hot spot and high temperature of heat sources. Seri Lee has developed an analytical simulation model for predicting and optimizing the thermal performance of bidirectional fin heat sinks [4]. As seen in Fig. 1. and Eq.(2.1)

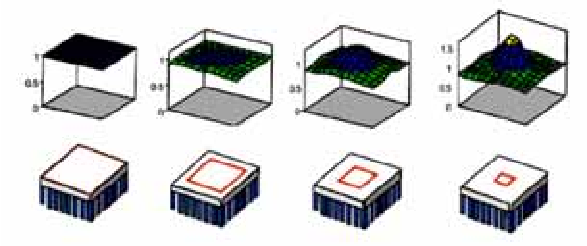

Fig1. Spreading thermal resistance of a heat sink

$$R_c = \frac{\sqrt{A_b} - \sqrt{A_s}}{k\sqrt{\pi A_b A_s}} \times \frac{\lambda k A_b R_o + \tanh(\lambda t)}{1 + \lambda k A_b R_o \tanh(\lambda t)} \tag{2.1}$$

$$\lambda = \frac{\pi^{3/2}}{\sqrt{A_b}} + \frac{1}{\sqrt{A_s}}$$

2.2 Surface temperature of multiple heat sources

As illustrated in Fig. 2 the spreader (such as vapor chamber) is of a×b dimension and the dual heat sources are arbitrarily located at the heat spreader surface. The analysis of the heat spreading on the multiple sources heating mode when the heat sources attached on surface of spreader, it is quite different from that of the single block-heating mode [5]. This is because the heat flow in the spreader is no longer one-dimensional. When the heat sources generate power on the spreader surface, there exists one-dimensional and lateral length spreading thermal resistance [6], thus, and heat conductivity field becomes three-dimensional instead.

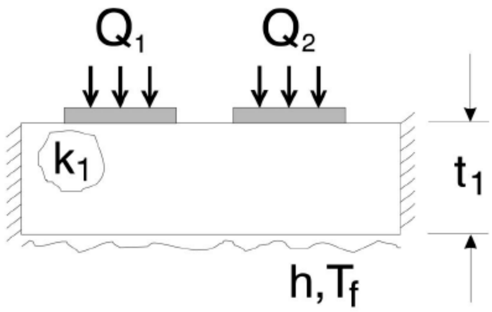

Fig. 2 Dual heat sources

2.3 Equivalent heat source calculation of LEDs

Distance (s) is introduced for this case, as Fig.3 shown, which describes the distance between the two LEDs with reference to the center (respectively. It is observed from this case that when the distance (s) is small, i.e. the two LEDs are placed close to one another near the center of the spreader. The maximum case temperature is the highest. Minimum temperature is determined on the plots that indicate the optimized positions of the LEDs on the spreader surface. Locations of the LEDs that allow optimum performance of the spreader must be determined.
Fig.4 and Eq.(2.2) shows Methodology of multiple heat sources to an equivalent heat source [7].

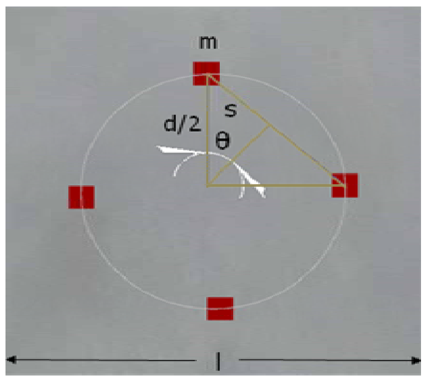

Fig. 3 Calculation of multiple LEDs to an equivalent heat source

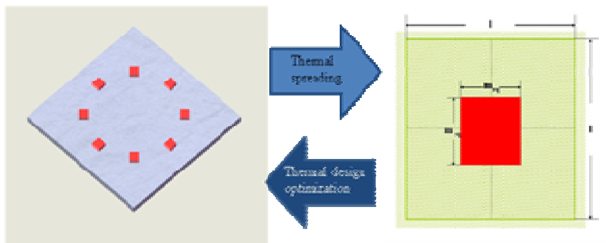

Fig.4 Methodology of multiple heat sources to an equivalent heat source

$$\frac{A_{eq}}{A} = \alpha \times \left(\frac{m}{l}\right)^{\beta} \times \left(\frac{s}{l}\sin\frac{\pi}{n}\right)^{\gamma} \tag{2.2}$$

$A_{eq} = f(l, m, s, n)$

d : Diameter between each two heat sources

s : Distance between each two heat sources
n : Number of heat sources
m : Heat source size
l : Spreader size
αβγ: Correlation factor of *f (l , m , s, n)*

3 Vapor chamber on Electronic Cooling Application

3.1 Performance Evaluation

The most versatile feature of using vapor chambers is the wide variety of geometries that can be constructed to take advantage of the available space around the electronics to be cooled. In many applications, the available heat sink size above the electronics is limited by the board-to-board spacing. In this situation, vapor chambers are used in a low profile design that equalizes the heat to a large fin stack.

In general, the smaller component (LEDs array) cooling approaches transport 10 to 30 W each. Most of these vapor chamber heat sinks use a 120mm * 90mm vapor chamber that eliminates hot spot. This type of passive design has been a very effective thermal management technique for LED with power ratings less than 30 W without cooling fan [8].

The optimal design helps to reduce airflow requirements and prevent one of the limiting factors is the volumetric airflow that current electronic system can produce reliably.

3.2 Experimental investigation

Experimental scenarios of quad heat sources thermal test are designed for leverage thermal test and numerical result, Fig. 5 shows the test procedures from heat sources distance 20mm to 50mm, it means heat spreading on the lateral length of a vapor chamber, which test plan is same as the numerical models [9]. Natural convection chamber provides a steady test environment of constant ambient air. [10].

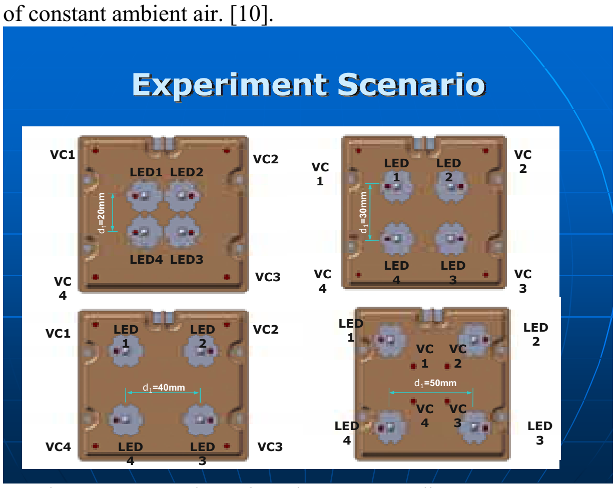

Fig.5 Test procedures from heat sources distance 20mm to 50mm

4 Numerical analysis

Based on the current capabilities of main CFD packages suitable for thermal design (such as FLOTHERM) and the nature of electronic applications [11], understanding the physics of the processes, introducing adequate simplifications and establishing an appropriate model are essential factors for obtaining reasonable results and correct thermal design [12].

With the Finite Difference Method (FDM)
Verifying thermal design such as:

- Heat sources power dissipation
- Convection variation
- Thermal resistance
- Local ambient temperature
- Processor heat sink design

Vapor chambers can be installed in the base of an extrusion to reduce the conduction spreading resistance. Spreading resistance occurs when a heat source's chip area is smaller than that of the heat sink's base.

Fig.6 shows a spreader (240×240×4mm [LWH]) that was tested using natural convection (Open air and air inlet temperature around 25℃) with a heat source size of 15×15 mm and a power dissipation of 3W.

The temperature profiles at the surface of metal spreader and vapor chambers appear in Fig.6 respectively. The shape of the temperature profiles in Fig. 6 demonstrates that heat spreader temperature. With vapor chamber assisted heat sink; thermal engineers can place the electrical components in convenient locations and is not limited by spreading resistance to the center of the heat sink [13].

As shown in Fig. 7, the vapor chambers also significantly reduced the maximum surface temperature of the extrusion. By simply adding vapor chambers to the base of an existing heat sink, the overall sink to ambient temperature rises are reduced by 30%. Faced with high spreading resistance, the thermal designer would probably explore the feasibility of increasing the base thickness in an effort to reduce both the heat transfer by conduction and mass [14].

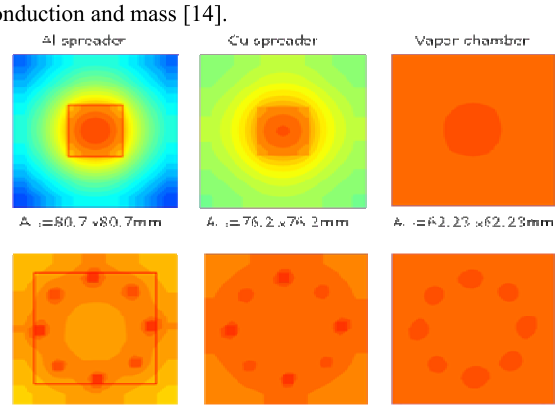

Fig. 6 Experiment description

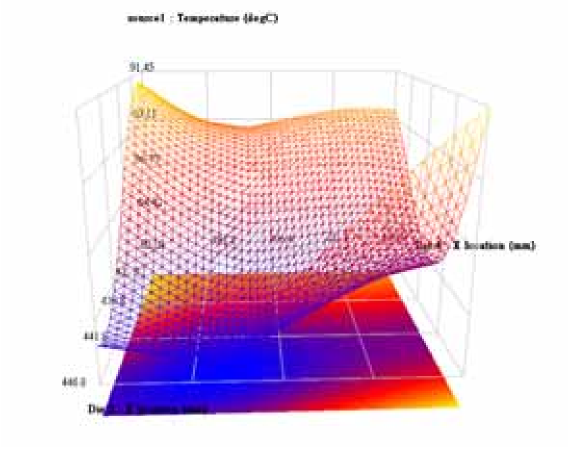

Fig.7 Surface temperature for an equivalent heat source

5 Conclusion

This study shows a progression of cooling approaches advance thermal design, which growing heat dissipation levels of LED devices. Vapor chamber assemblies (low heat dissipation from 10 to 30W) allow increased heat sink performance within the volume available with little potential impact on the existing system design.

Vapor chambers are now being combined with other technology to help meet the emerging requirements. In practice, these cooling units might be the best solutions for keeping pace with the increasing heat loads of high power semiconductors [15]. The reliability and flexibility of the vapor chamber has proven to be a valuable attribute that provides the system designer with increased LED layout possibilities and typically improves thermal performance. The fin stack height, width, length, and fin spacing can be calculated by CFD numerical optimization. Electronic system also can be customized to fit the application [16].

6 REFERENCES

[1] Y.S. Chen, K.H. Chien, T.S. Hung, C.C. Wang, Y.M. Ferng, B.S. Pei, Numerical simulation of a heat sink embedded with vapor chamber and calculation of effective thermal conductivity of a vapor chamber, Journal of Applied Thermal Engineering, 2008

[2] Faghri, Amir, Heat pipe science and technology, Taylor & Francis, 1995.

[3]Yu, C.S., Wei, W.C., Kang, S.W.," Investigation of Micro Porosity Sintered Wick in Vapor Chamber for Fan Less Design." Thermal Investigation of ICs and Systems, 2007. IEEE THERMINIC 2007. 13th International Workshop on Volume, Issue, 17-19, pp.88 – 91, 2007.

[4]Song S., Lee, S. and Au, V., "Constriction/Spreading Resistance Model for Electronic Packaging", Proceedings of the 4th ASME/JSME thermal Engineering Joint Conference, 4, pp. 199-206, 1995.

[5] Muzychka, Y.S., Culham, J.R. and Yovanovich, M.M., Thermal Spreading Resistance of Eccentric Heat Sources on Rectangular Flux Channels, ASME, J. Electronic Packing, 125, pp. 178-185, 2003.

[6] Kennedy, D.P., Spreading Resistance in Cylindrical Semiconductor Devices, J. Applied Physics, 31, pp. 1490-1497, 1960.

[7] Yun Ho Kim, Seo Young Kim, Gwang Hoon Rhee, "Evaluation of spreading thermal resistance for heat generating multi-electronic components", Thermal and Thermomechanical Phenomena in Electronics Systems, ITHERM 2006-June 2, pp. 264, 2006.

[8] A. Faghri, M. Buchko, Experimental and numerical analysis of low temperature heat pipes with multiple heat sources, ASME Journal of Heat Transfer 113 728-734. 1991

[9] Zuo, Z. J. and Faghri, A., A network thermodynamic analysis of the heat pipe, Int. J. Heat Mass Transfer, vol. 41, pp. 1473-1484, 1998.

[10] Tournier, J. M. and El-Genk, M. S., A heat pipe transient analysis model, Int. J. Heat Mass Transfer, vol. 37, pp. 753-762, 1994.

[11] HTTP://WWW.FLOTREND.COM.

[12] CFD Molding of a Therma-Base Heat Sink, Thermacore, Inc., 1998

[13] Vadakkan, Unnikrishnan, Garimella, Suresh V. and Murthy, Jayathi Y., Transport in Flat Heat Pipes at High Heat Fluxes from Multiple Discrete Sources, J. Heat Transfer, vol. 126, pp.347-354, June 2004.

[14] Koito, Y., Imura, H., Mochizuki, M., Saito, Y., and Torii, S, Numerical analysis and experimental verification on thermal fluid phenomena in a vapor chamber, Applied Thermal Engineering, vol. 26, pp. 1669-1676, 2006.

[15] Tan, B. K., Huang, X. Y., Wong, T. N. and Ooi, K. T., A study of multiple heat sources on a flat plate heat pipe using a point source approach, Int. J. Heat Mass Transfer, vol. 43, pp. 3755-3764, 2000.

[16] Zhu, N. and Vafai, K., Vapor and liquid flow in an asymmetrical flat plate heat pipe: a three-dimensional analytical and numerical investigation. Int. J. Heat Mass Transfer, vol. 41, pp. 159-174, 1998